A Miniaturized High-Voltage Solar Cell Array as an Electrostatic MEMS Power Supply

Jeong B. Lee, Zhizhang Chen, Mark G. Allen, *Member, IEEE,* Ajeet Rohatgi, *Fellow, IEEE,* and Rajeewa Arya

***Abstract*—A hydrogenated amorphous silicon (a-Si:H) solar cell array that is designed as an on-board power source for electrostatic microelectromechanical systems (MEMS) is presented. A single cell consists of a triple layer of *p-i-n/p-i-n/p-i-n* a-Si:H and produces an open circuit voltage (V_{oc}) of 1.8~2.3 V, a short circuit current density (J_{sc}) of 2.8 mA/cm^2, and fill factor (FF) of 0.495. A series interconnected array of 100 single solar cells (total array area of 1 cm^2) is fabricated in an integrated fashion and produces an array V_{oc} of 150 V, and array short circuit current (I_{sc}) of 2.8 μA under Air Mass (AM) 1.5 illumination. To demonstrate the usefulness of this solar cell array as an on-board power source for electrostatically driven micromachined devices, it has been packaged with a movable micromachined silicon (Si) mirror in a hybrid manner. The movable Si mirror is directly driven by the cell array electrical output, and the motion of the mirror plate has been observed reproducibly. Variation of light intensity and/or number of illuminated cells produces different values of array V_{oc}, thus enabling control of the deflection of the Si mirror by variation of incident light intensity. [117]**

I. Introduction

SINCE THE power requirements of micromachined devices are usually quite different from those of general electrical circuitry, additional external power connections or voltage/current conversion circuitry are commonly used in microelectromechanical systems (MEMS). In many applications, these methods of power supply are not a problem; however, for autonomous operation, such as free-moving microrobotic systems and space-based MEMS, a self-contained on-board or remote power supply is desirable. Previous work in this area includes a rechargeable lithium microbattery [1] that can be used as a self-contained on-board power supply; an energy coupling method using an external magnetic field to remotely induce voltages and currents on-chip [2]; and dielectric loss heating by means of a remote electric field alternating at high frequency [3]. Solar cells are also attractive as power sources for MEMS since they are easily integrated and, therefore, can be fabricated as a self-contained on-board power supply. In addition, solar cells are very well characterized and developed in many terrestrial, space, and commercial applications. However, to be used as power sources for MEMS, a suitable modification in the traditional design methodology of the solar cell is required to meet the power requirements of MEMS.

The power requirements of MEMS differ depending on the actuation principle involved. Common driving principles currently used for MEMS include electrostatic [4], magnetic [5], piezoelectric [6], and electrothermal [7] excitation. Typical power requirements of these driving principles are shown in Table I. Although some researchers have succeeded in decreasing the driving voltage of some electrostatic MEMS [8], these devices usually require driving voltages ranging from tens to hundreds of volts and driving currents in the nA~μA range. These voltages and currents are different from those traditionally available from solar cells, which are lower-voltage supplies. Thus, as discussed, a suitable modification in the traditional design is required. This paper consists of design criteria for solar cells as a power source for electrostatic MEMS, solar cell array fabrication, experimental results for a single cell, a series interconnected cell array, and an actuation demonstration using the cell array to drive a micromachined movable silicon (Si) mirror [9].

Manuscript received June 22, 1994; revised April 4, 1995. This work was supported in part by the National Science Foundation under grant ECS-9117074. Subject Editor, A. P. Pisano.

J. B. Lee, M. G. Allen, and A. Rohatgi are with the School of Electrical and Computer Engineering, Microelectronics Research Center, Georgia Institute of Technology, Atlanta, GA 30332-0250 USA.

Z. Chen was with the School of Electrical and Computer Engineering, Microelectronics Research Center, Georgia Institute of Technology, Atlanta, GA 30332-0250 USA. He is now with Siltec Silicon Corporation, Salem, OR 97303 USA.

R. Arya is with Solarex Corporation, Newtown, PA 18940 USA.

IEEE Log Number 9412348.

II. Principle of Operation of Solar Cell

A solar cell is a device producing electrical energy directly from light energy. The basic device requirement of a solar cell is an electronic asymmetry, such as a *p-n* junction. When illuminated, photogenerated electron-hole pairs (EHP) are generated throughout the solar cell. If the cell is connected to a load, current will flow from one region of the cell, through the load, and back to the other region of the cell. Fig. 1 shows an I-V characteristic curve for dark and illuminated conditions for a simple p-n junction. The I_{mp} and V_{mp} are the current and voltage operating point for maximum power output. An important solar cell parameter, the fill factor (FF), is defined as

$$\mathrm{FF} = \frac{I_{mp}V_{mp}}{I_{sc}V_{oc}} \tag{1}$$

where I_{sc} is the short circuit current and V_{oc} is the open circuit voltage as defined in Fig. 1. The efficiency of a solar cell is defined as

$$\eta = \frac{I_{mp}V_{mp}}{P_{in}} = \frac{\mathrm{FF}\cdot I_{sc}\cdot V_{oc}}{P_{in}} \tag{2}$$

where P_{in} is the input optical power to the solar cell.

TABLE I
COMMON DRIVING PRINCIPLES IN MICROMACHINING AND THEIR POWER REQUIREMENTS

Device	Driving Principle	Material	Power Requirement	Reference
Motor	Electrostatic	poly-Si	60~400 V / nA ~ μA	[4]
Motor	Magnetic	Ni-Fe	~ 1V / 500 mA	[5]
Motor	Piezoelectric	PZT	4V (100 kHz) / ~ μA	[6]
Actuator	Electrothermal	Si/Au	~ 10 V / ~ mA	[7]

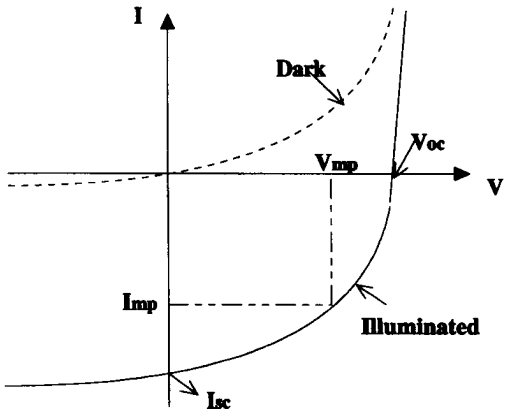

Fig. 1. I-V characteristic curve for a simple p-n junction under dark and illuminated conditions.

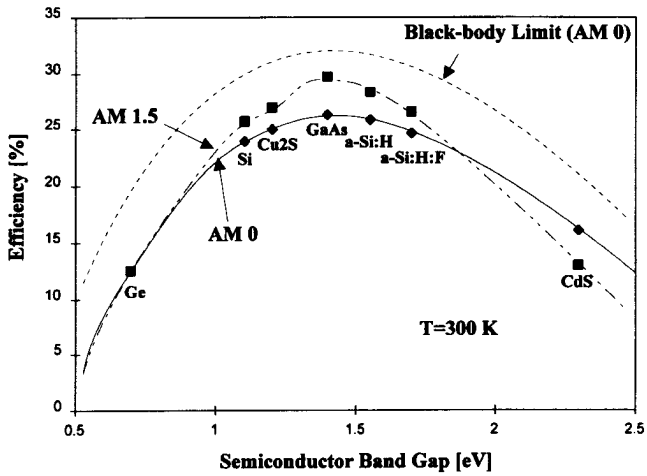

Fig. 2. Solar cell efficiency limits as a function of the band gap of the cell material [10].

III. DESIGN CRITERIA

Several design criteria for solar-cell-based MEMS power sources arise from the basic design rules of micromachining. First, the solar cell should consume as small an area as possible in order to minimize the overall size of the MEMS. Second, the solar cell should be electrically isolated from the substrate to allow an isolated integration of microsensors, microactuators, electrical circuitry, and the solar cell power supply. Third, the fabrication processes should be fully or partially compatible with each other. Additional design criteria arise from the power requirements of electrostatic MEMS. First, the individual cells must be able to be connected in series with each other so that the interconnected cell array can meet the high driving voltage requirement. Second, a high V_{oc} of a single cell is desirable. Note that in contrast to usual solar cell design criteria, maximization of the cell current and/or array current is not required since the typical driving current for electrostatic MEMS is in the nA~μA range. In order to facilitate series interconnection of cells, it is necessary to be able to make a connection from the bottom of one cell to the top of the next cell. Therefore, thin film solar cells may be preferred in order to meet this criterion. For the electrical isolation design, thin film solar cells are preferred once again since the electrical isolation of a thin film structure is much easier than a bulk wafer-type solar cell.

To make an efficient solar cell, it is necessary to provide for absorption of a large fraction of incident light, efficient collection of photogenerated EHP's, low internal series resistance, and low leakage current. These requirements are closely related to material properties. As the band gap decreases, J_{sc} increases because more photons can generate EHP's. The V_{oc}, however, decreases with decreasing band gap. Thus, there is an optimum band gap semiconductor for the highest efficiency. Fig. 2 [10] shows the solar cell efficiency limits for solar illumination for popular contemporary photovoltaic (PV) materials as a function of the band gap of the material. The peak efficiency occurs from 1.4 to 1.6 eV. Another important property in PV materials is the optical absorption coefficient $\alpha(\lambda)$, which is a function of the wavelength of the incident light. If the $\alpha(\lambda)$ is high, a relatively thin structure is sufficient to absorb most of the incident light. This thin structure has the added advantage that a relatively short minority carrier diffusion length of the photogenerated EHP's is required for the minority carriers to reach the junction without recombination.

Table II shows output characteristics and typical thicknesses for various contemporary solar cells. Although the single crystal Si solar cell is the most common in PV technology and has a high J_{sc} and PV conversion efficiency, it has a relatively low $\alpha(\lambda)$. Thus, solar cells formed from this material have typical thickness of 200~400 μm. Therefore, single crystal Si solar cells are usually formed in a bulk wafer, resulting in a failure to meet the design criteria discussed. The polycrystalline thin film Si solar cell has relatively low V_{oc}. Single-layer gallium arsenide (GaAs) and two terminal tandem GaAs solar cells have high V_{oc} in a single cell and can be realized as a thin film; however, GaAs is more expensive than the other materials. The cadmium telluride (CdTe)-based solar cells also have low V_{oc}. Taking into account several basic material properties, the hydrogenated amorphous silicon (a-Si:H) solar cell is a very attractive means to realize an on-board power supply for electrostatic MEMS for several

TABLE II
TYPICAL PARAMETER SUMMARY OF THE MAJOR CONTEMPORARY SOLAR CELLS

Solar Cell	Voc [V]	Jsc [mA/cm^2]	η [%]	Thickness [μm]	Reference
Single crystal Si	0.7	41	23	200 ~ 400	[11]
Thin film poly-Si	0.6	33	15.7	~ 30	[12]
GaAs	1.045	27.6	24.4	2 ~ 10	[13]
Two terminal tandem GaAs	2.403	13.96	27.6	2 ~ 10	[13]
Triple layer a-Si	2.541	6.96	12.4	~ 1	[13]
CdS/CdTe	0.446	31.1	8.1	~ 30	[14]

reasons. First, since it has a relatively large band gap (about 1.55 eV, depending on the hydrogen concentration), cells made from this material have a high V_{oc} of about 0.9 V. Second, the $\alpha(\lambda)$ of a-Si:H is more than an order of magnitude larger than that of single crystal Si near the maximum solar photon energy region of 500 nm. Accordingly, the optimum thickness of the active layer in a-Si:H solar cells can be on the order of 1 μm, much smaller than that of single crystal Si solar cells. Third, it is possible to stack multiple layers of a-Si:H to realize tandem cells for high voltage output and very efficient utilization of substrate area. Finally, since a-Si:H can be deposited using dc glow discharge decomposition and RF sputtering, it can be deposited on virtually any low cost substrate, thereby enabling cost-effective processing.

IV. A HYDROGENATED AMORPHOUS SILICON SOLAR CELL

Since Carlson and Wronski [15] reported the first a-Si:H solar cells, there have been tremendous efforts and improvements. The primary reason for the popularity of this material is the capability to fabricate devices at low cost. Due to the deposition technology which has been developed for a-Si:H solar cells, this material can be deposited virtually on any low cost substrate. In order to achieve high efficiency cells, multijunction-type a-Si solar cells have been proposed. Horizontally [16] and vertically [17] stacked multilayer solar cells have both been introduced in which a single cell has a V_{oc} in excess of 2 V. In theory, the larger the number of cells in a vertical stack, the larger the overall V_{oc} of the stack. However, in large number stacks, the thicknesses of the i-layers and the junction band gaps should be carefully designed [18] to achieve a high efficiency, so that the cells on the bottom of the stack contribute to the overall power generation. In this work, the vertically stacked triple junction cell has been investigated, since it is the most popular cell used in multijunction a-Si solar cells and therefore well characterized. These individual cell stacks are then interconnected horizontally in series to produce an array of high voltage output. The major disadvantage of a-Si as a material is the instability of the cell performance during the PV operation. Cells of a-Si exhibit degradation in performance after exposure to light, known as Staebler-Wronski effect [19]. In general, most of the degradation is observed in the first 48 hours of operation, and is accompanied by a drop in efficiency (η) of 15 ~ 25%, due to a degradation of J_{sc} and FF [13]. However, V_{oc} is fairly stable [13], which is the most important criterion for electrostatic MEMS as the operating current is relatively low. There is a large literature on the long-term stability of a-Si-based solar cell [20], [21]. Another major issue of the a-Si:H solar cell in a MEMS application is the temperature limitation. The a-Si:H film begins to lose hydrogen at temperatures exceeding 400°C, irreversibly damaging the PV performance. Several MEMS fabrication processes do not exceed this temperature limit (such as electroplating- based processes [22], [23]); however, many of the common polycrystalline silicon processes will require the solar cell material to be deposited after the polysilicon deposition.

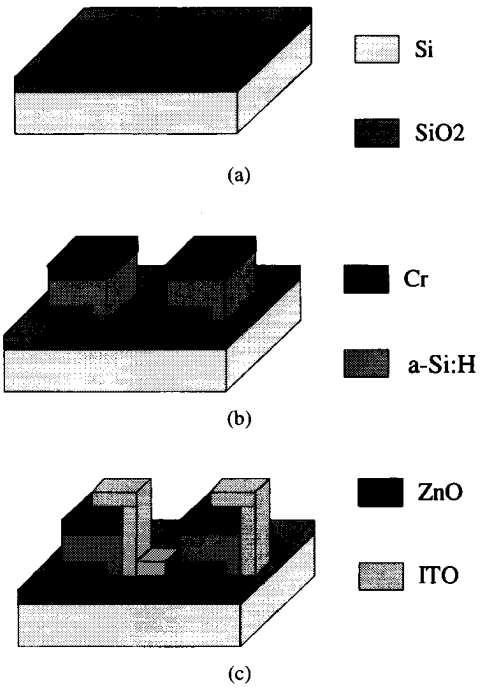

Fig. 3. The fabrication process of triple junction solar cell array. (a) Cr rear contact; (b) a-Si:H triple junction solar cell and anti-reflective coating; (c) ITO interconnection patterning (figures are not to scale).

V. FABRICATION

A brief fabrication process of the solar cell array is shown in Fig. 3. The process begins with a 3-in. ⟨100⟩ Si wafer as a substrate. A 4000 Å layer of silicon dioxide (SiO_2) for electrical isolation is deposited onto the Si wafer by plasma enhanced chemical vapor deposition (PECVD) using silane (SiH_4) and nitrous oxide (N_2O). A 1-μm layer of chromium (Cr) is deposited onto the SiO_2 layer by dc sputtering. The Cr layer is patterned using 50% hydrochloric acid (HCl) to

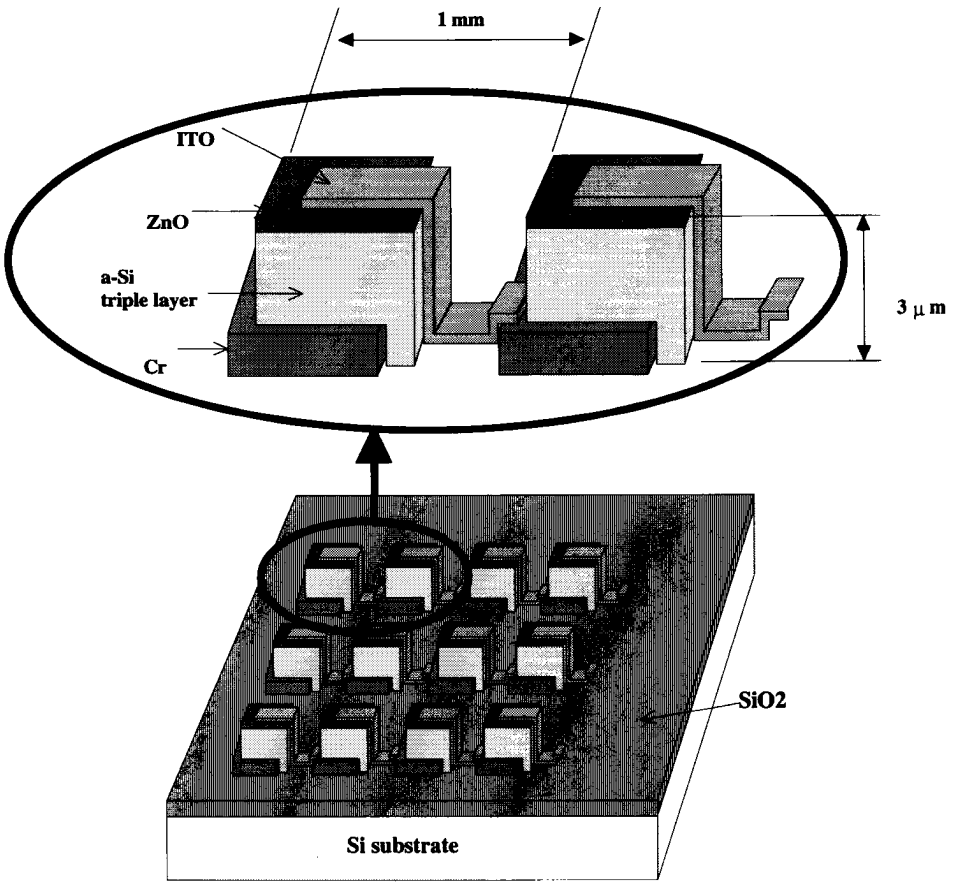

Fig. 4. The schematic diagram of series interconnected a-Si:H solar cell array.

form a rear contact. A total of 1 μm of a-Si:H *p-i-n/p-i-n/p-i-n* triple junctions are deposited by dc glow-discharge decomposition of SiH_4, diborane (B_2H_6), methane (CH_4) for the p-layer, SiH_4 for the i-layer, and SiH_4, phosphine (PH_3) for the n-layer, respectively. A zinc oxide (ZnO) anti-reflective coating (ARC) layer is deposited on top of the a-Si triple-stacked layers and is patterned using 10% HCl. The ARC is a transparent, electrically conducting layer and has been designed to improve the light absorption by preventing light reflection from the air/a-Si cell interface. Detailed design considerations for ARC's are available [10], [24]. The a-Si:H is then mesa etched in a 100% carbon tetrafluoride (CF_4) plasma at 150 W incident power. A 1200-Å layer of indium tin oxide (ITO) is deposited using RF sputtering, and is patterned using 5% hydrofluoric acid (HF). The ITO layer is optically transparent and form a series electrical interconnection between individual cells. The sample is then annealed at 220°C for 20 min. in a rapid thermal processor (RTP) system to decrease the sheet resistance of the ITO. Fig. 4 shows the series interconnected cell array in detail.

VI. Experiments

A. Triple-Stacked Single-Tandem Cell

Vertically triple-stacked single test cells with area of 0.1 cm^2 were fabricated as described above and characterized under near AM 1.5 conditions (the AM 1.5 condition is the standard solar cell test light intensity and energy distribution condition, which corresponds to illuminated sunlight on the surface of the earth when the sun is at an inclination of 48.19° relative to overhead). A typical I-V characteristic curve of single cell is shown in Fig. 5. The V_{oc} is in the range of 1.8 $\sim$ 2.3 V, the short circuit current density J_{sc} is about 2.8 mA/cm^2, and the fill factor (FF) is 0.495. As shown in Fig. 5, the FF is low, in part due to the Cr rear contact, which may diffuse into the a-Si:H active layer during the dc glow-discharge decomposition at 250°C, resulting in lower FF and lower V_{oc}. Different metals are planned for use as a rear contact, such as titanium (Ti), to reduce this effect and improve V_{oc}. The J_{sc} can be improved further by using an efficient ARC and i-layer thickness optimization.

B. Series-Interconnected Solar Cell Array

After making series interconnection between individual solar cells as described above, the array V_{oc} was measured under varying light conditions. The array V_{oc} measurements were carried out using a Keithley 236 Source Measurement Unit, which has a very high input impedance to prevent any voltage drop during the voltage measurement due to loading effects. The array V_{oc} as a function of the number of cells in series under varying illuminations is shown in Fig. 6. As expected, the array V_{oc} is linearly proportional to the number of cells in

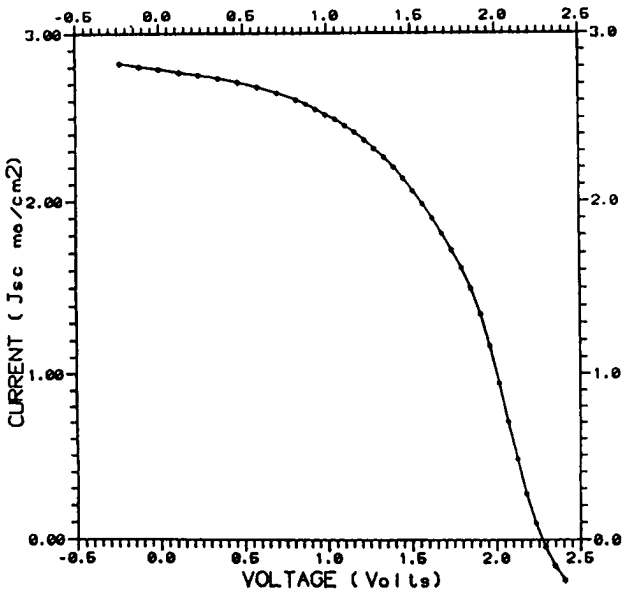

Fig. 5. The I-V characteristic curve for triple-stacked single a-Si:H solar cell.

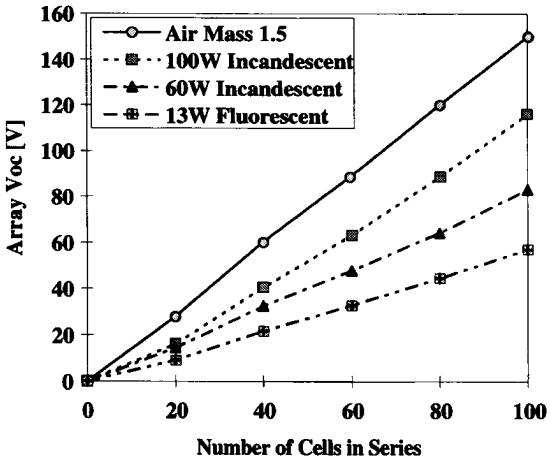

Fig. 6. Array V_{oc} as a function of number of cells in array, under AM 1.5, 100-W incandescent light bulb/40 cm apart, 60-W incandescent light bulb/40 cm apart, 13-W fluorescent lamp/40 cm apart, respectively.

the array. For a 100-cell series-interconnected array (total array area of 1 cm^2), the measured V_{oc} is as high as 150 V under AM 1.5 condition. Even under the relatively poor illumination of a 13-W fluorescent lamp, which is located at 40 cm above the cell array, a V_{oc} of 57 V was attained.

For a 100-cell series-interconnected array (total array area including interconnections of 1 cm $\times$ 1 cm, and total amorphous silicon area of 6 mm $\times$ 6 mm), the measured I_{sc} is 2.8 μA under AM 1.5 illumination. The sheet resistance of the ITO after annealing is about 20 Ω/square. The calculated resistivity of the ITO in the cell array is (20 Ω/square) $*$ (1200 Å) = 240 $\mu\Omega$-cm. With this sheet resistance value, the power available from the cell is reduced in the worst case (i.e., maximum current being drawn from the cell) by 12%. At low current values, this efficiency loss is correspondingly reduced.

When the number of series interconnected cells in the array is kept constant, the array V_{oc} increases as the light intensity increases. The variation of array V_{oc} as a function of

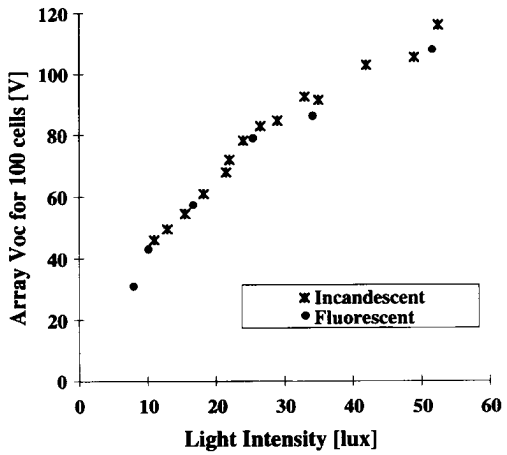

Fig. 7. Array V_{oc} as a function of photometric light intensity, which has been carried out by varying the distance between light sources and cell array.

light intensity variation (actually varying the distance between the cell array and the light source) has been measured by using a PASCO 9152B photometer. Fig. 7 shows the resultant V_{oc} as a function of illuminance (lux) under varying light sources, where 1 lux is equal to 1 lm/m^2 at a wavelength of 560 nm [25]. Even though the spectral response of the photometer does not exactly match that of the incandescent and fluorescent lamps, the measured light intensities give relative references. The illumination engineering society recommends that 100 lux for normal lighting in ordinary residences. Based on this recommendation, the 100-cell series-interconnected array can produce above 100 V either under the incandescent lamp or fluorescent lamp in an ordinary residential area. The results described in Figs. 6 and 7 illustrate that the solar cell array developed in this paper is applicable as a high voltage power supply for many electrostatically driven micromachined devices even under ordinary room light conditions.

C. Demonstration of Electrostatic MEMS Operation

The series-interconnected array of one hundred a-Si:H solar cells was bonded and packaged on a standard flat-pack carrier with a micromachined movable Si mirror suspended at its center by flexible polyimide supports [9]. The photomicrograph of the packaged device is shown in Fig. 8(a). The movable Si mirror is directly driven by the electrical output of the solar cell array. The driving voltage from the cell array is placed between the electrode on top of the movable Si mirror plate and the underlying metallic surface (ground) of the flat-pack carrier. A polyimide (Kapton) tape has been placed underneath the suspended Si mirror to prevent electrical shorting between the Si mirror plate and the bottom ground. The deflection of the tip of the Si mirror was measured by focusing on the tip of the mirror using a Nikon MM-11 Measurescope and measuring the deflection of the microscope head necessary to keep the deflecting tip in focus. Motion of the Si mirror plate was observed from approximately 63 V array output. As expected for this type of electrostatically driven capacitive actuator, the deflection of the tip of the mirror is linearly proportional to the square of the output voltage of the cell

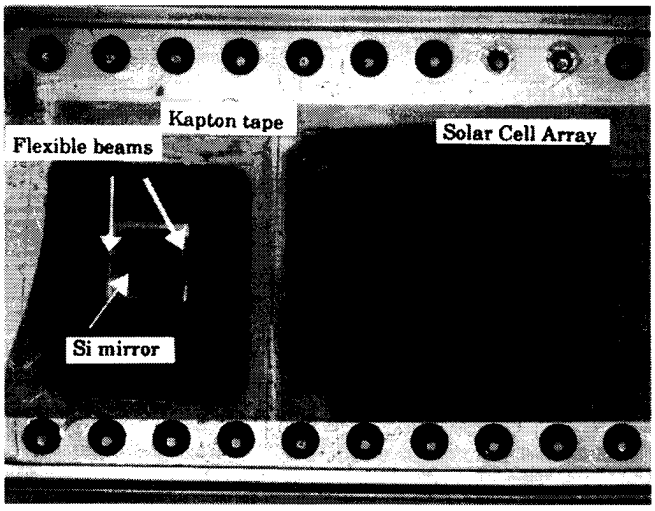

(a)

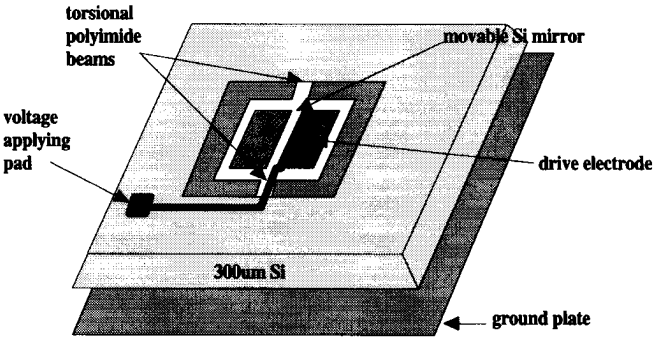

(b)

Fig. 8. (a) A photograph of a series interconnected 100-cell array (total array area of 1 cm^2) packaged with a movable Si mirror. (b) A schematic diagram of the movable Si mirror.

array up to 105 V (where the voltage variation was obtained by varying the position of the light source relative to the cell array), at which time the movable Si mirror plate snapped to the bottom electrode. The detailed plot of the deflection of the tip of the mirror is shown in Fig. 9. This behavior could be reproducibly observed.

VII. Conclusion

An a-Si:H solar cell array with multiple number of cells interconnected in series has been designed, fabricated, characterized, and demonstrated as an on-board power supply for an electrostatically driven micromachined device. The electrical output characteristics of the solar cell array are well matched to the power requirements of electrostatic MEMS. An open circuit voltage as high as 150 V and a short circuit current of 2.8 μA under AM 1.5 conditions has been achieved by this small size (1 cm^2) solar cell array. Variation of the incident light intensity produces an adjustable array V_{oc}, thus allowing control of electrostatic actuation by changing the incident light intensity. This solar cell array can also be used as power supply for any device that requires voltages ranging from several to above 100 V with small currents in the nA $\sim\mu$A range.

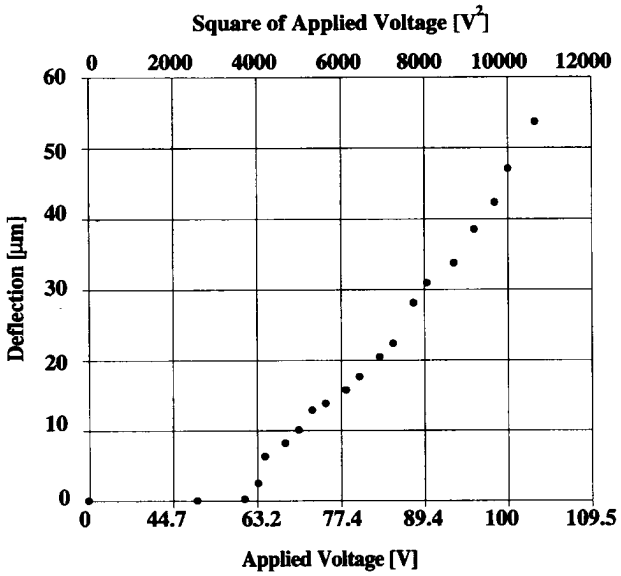

Fig. 9. Deflection of the tip of the Si mirror as a function of square of applied output voltage of an a-Si:H solar cell array.

Acknowledgment

Microfabrication, except as noted below, was carried out at the Georgia Tech. Microelectronics Research Center. The support of the staff of the Pettit Microelectronics Research Center at Georgia Tech. is acknowledged. The amorphous silicon deposition was carried out at Solarex, Inc., and the fabrication of the micromachined Si mirror was carried out at the Massachusetts Institute of Technology. Valuable technical discussions with Prof. C. H. Ahn at the University of Cincinnati, Prof. A. Bruno Frazier at Louisiana Tech., and Mr. M. H. Lee at Georgia Tech. are greatly appreciated.

References

[1] J. B. Bates, G. R. Gruzalski, and C. F. Luck, "Rechargeable solid state lithium microbatteries," in *Proc. 6th IEEE Workshop on Micro Electro Mechanical Systems*, Fort Lauderdale, FL, Feb. 1993, pp. 82–86.

[2] H. Matsuki *et al.*, "Implantable transformer for an artificial heart utilizing amorphous magnetic fibers," *J. Appl. Phys.*, vol. 64, pp. 5859–5861, 1988.

[3] B. Rashidian and M. G. Allen, "Electrothermal microactuators based on dielectric loss heating," in *Proc. 6th IEEE Workshop on Micro Electro Mechanical Systems*, Feb. 1993, Fort Lauderdale, FL, pp. 24–29.

[4] L. S. Fan, Y. C. Tai, and R. S. Muller, "IC-processed electrostatic micromotors," *Sensors and Actuators*, vol. 20, no. 1–2, pp. 41–47, Nov. 1989.

[5] C. H. Ahn, Y. J. Kim, and M. G. Allen, "A planar variable reluctance magnetic micromotor with fully integrated stator and coils," *J. Microelectromechanical Syst.*, vol. 2, no. 4, pp. 165–173, Dec. 1993.

[6] A. M. Flynn, L. S. Tavrow, S. F. Bart, R. A. Brooks, D. J. Ehrlich, K. R. Udayakumar, and L. E. Cross, "Piezoelectric micromotors for microrobots," *J. Microelectromechanical Syst.*, vol. 1, no. 1, pp. 44–51, Mar. 1992.

[7] W. Riethmuller and W. Benecke, "Thermally excited silicon microactuators," *IEEE Trans. Electron Dev.*, vol. 35, no. 6, pp. 758–763, June 1988.

[8] T. Hirano, T. Furuhata, K. J. Gabriel, and H. Fujita, "Design, fabrication, and operation of submicron gap comb-drive microactuators," *J. Microelectromechanical Syst.*, vol. 1, no. 1, pp. 52–59, Mar. 1992.

[9] M. G. Allen, M. Scheidl, R. L. Smith, and A. D. Nikolich, "Movable micromachined silicon plates with integrated position sensing," *Sensors and Actuators*, vol. A21, no. 1–3, pp. 211–214, Feb. 1990.

[10] M. A. Green, *Solar Cells: Operating Principles, Technology, and System Applications*. Englewood Cliffs, NJ: Prentice-Hall, 1982, p. 89.

[11] M. A. Green, S. R. Wenham, and J. Zhao, "Progress in high efficiency silicon cell and module research," in *Proc. 23rd IEEE Photovoltaic Specialists Conf.*, Louisville, KY, 1993, pp. 8–13.
[12] A. M. Barnett, F. A. Domian, B. W. Feycock, D. H. Ford, C. L. Kendall, J. A. Rand, T. R. Ruffins, M. L. Rock, and R. B. Hall, "Developments of large area thin crystalline silicon-film solar cells," in *Proc. 20th IEEE Photovoltaic Specialists Conf.*, Las Vegas, NV, 1988, pp. 1569–1574.
[13] L. L. Kazmerski, "Status and assessment of photovoltaic technologies," *Int. Materials Rev.*, vol. 34, no. 4, pp. 185–210, 1989.
[14] H. Uda, H. Matsumoto, Y. Komatsu, A. Nakano and S. Ikegami, "All screen printed CdS/CdTe solar cell," in *Proc. 16th IEEE Photovoltaic Specialists Conf.*, 1982, pp. 801–804.
[15] D. E. Carlson and C. R. Wronski, "Amorphous silicon solar cell," *Appl. Phys. Lett.*, vol. 28, no. 11, pp. 671–673, June 1976.
[16] Y. Hamakawa, H. Okamoto, and Y. Nitta, "A new type of amorphous silicon photovoltaic cell generating more than 2.0 V," *Appl. Phys. Lett.*, vol. 35, no. 2, pp. 187–189, July 1979.
[17] S. Guha *et al.*, "A novel design for amorphous silicon alloy solar cells," in *Proc. 20th IEEE Photovoltaic Specialists Conf.*, 1988, pp. 79–84.
[18] D. E. Carlson, "Multijunction amorphous silicon solar cells," *Philosophical Mag. B*, vol. 63, no. 1, pp. 305–313, 1991.
[19] D. L. Staebler and C. R. Wronski, "Reversible conductivity changes in discharge-produced amourphous silicon," *Appl. Phys. Lett.*, vol. 31, no. 4, pp. 292–294, Aug. 1977.
[20] R. R. Arya, L. Yang, M. Bennett, J. Newton, Y. M. Li, B. Fieselmann, L. F. Chen, K. Rajan, G. Wood, C. Poplawski, and A. Wilczynski, "Recent improvements in amorphous silicon-based multijunction modules," in *Proc. AIP Conf.* , 1994, no. 303, pp. 120–126.
[21] R. E. I. Schropp, M. B. von der Linden, J. D. Ouwens, and H. de Gooijer, "Apparent gettering of the Staebler-Wronski effect in amorphous silicon solar cells," *Solar Energy Materials and Solar Cells*, vol. 34, no. 1–4, pp. 455–463, Sept. 1994.
[22] E. W. Becker *et al.*, "Fabrication of microstructures with high aspect ratios and great structural heights by synchrotron radiation lithography, galvanoformung, and plastic moulding (LIGA process)," *Microelectronic Engineering*, vol. 4, pp. 35–56, 1986.
[23] A. B. Frazier and M. G. Allen, "Metallic micro-structures fabricated using photosensitive polyimide electrplating molds," *J. Microelectromechanical Syst.*, vol. 2, no. 2, pp. 87–94, June 1993.
[24] R. A. Hartman, P. E. Koch, and G. C. Catella, "Design considerations for an amorphous silicon modules," in *Proc. 18th IEEE Photovoltaic Specialists Conf.*, Las Vegas, NV, USA, Oct. 1985, pp. 1190–1194.
[25] F. L. Pedrotti, S. J. Leno, and S. Pedrotti, *Introduction to Optics*. Englewood Cliffs, NJ: Prentice-Hall, 1993, pp. 10–14.

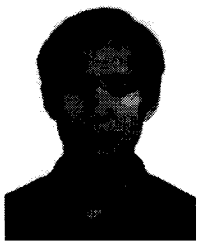

Jeong B. Lee received the B.S. degree in electronic engineering from the Hanyang University, Seoul, South Korea, in 1986, and the M.S. degree in electrical and computer engineering from Georgia Institute of Technology, Atlanta, in 1993. He is currently pursuing the Ph.D. degree in electrical and computer engineering at Georgia Tech.

His research interests include miniature on-board power systems for MEMS, design and fabrication of remotely controlled micromachined systems, finite element modeling, and multichip module (MCM).

Zhizhang Chen received the B.S. and M.S. degrees in electronics from Nankai University, China, in 1982 and 1985 respectively; the M.S. degree in physics from Oregon State University in 1987; and the Ph.D. degree in material engineering from Virginia Polytechnic and State University, Blacksburg, VA, in 1991.

In 1991 he joined the research faculty of the Microelectronics Research Center at Georgia Tech. His research interests are semiconductor device related thin film processes, including PECVD, APCVD, and LPCVD. He has 30 publications in semiconductor material and device research. Since 1995, he has worked at Siltec Silicon Corporation, Salem, Oregon, as a Senior Process Engineer in thin films.

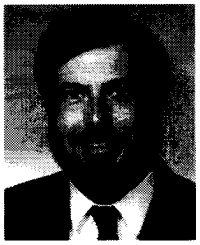

Mark G. Allen (M'89) received the B.A. degree in chemistry, the B.S.E. degree in chemical engineering, and the B.S.E. degree in electrical engineering from the University of Pennsylvania in 1984, the S.M. degree from the Massachusettes Institute of Technology in 1986, and the Ph.D. degree from MIT in 1989.

Since 1989 he has been at Georgia Institute of Technology where he currently holds the rank of the Associate Professor. His research interests include micromachining fabrication technology, microoptomechanical systems, and material issues in micromachined structures and electronic packages.

Dr. Allen is a member of the editorial board of the *Journal of Micromechanics and Microengineering*.

Ajeet Rohatgi (M'78–SM'86–F'91) received the B.S. degree in electrical engineering from Indian Institute of Technology, Kanpur, India, in 1971, the M.S. degree in materials engineering from Virginia Polytechnic Institute and State University, Blacksburg, in 1973, and the Ph.D. degree in metallurgy and material science from Lehigh University, Bethlehem, PA, in 1977.

Before joining the Electrical Engineering Faculty at Georgia Institute of Technology, Atlanta, in 1985, he was a Westinghouse Fellow at the Research and Development Center in Pittsburgh, PA. He is a Georgia Power Distinguished Professor in the School of Electrical and Computer Engineering and the Director of the University Center of Excellence for Photovoltaic Research and Education at Georgia Tech. His current research interests include modeling and fabrication of high-efficiency silicon and compound semiconductor solar cells; silicon MOS devices; semiconductor material and device characterization; defects and recombination in semiconductors; and MBE and MOCVD growth of compound semiconductors for optoelectronic and photovoltaic devices.

Dr. Rohatgi received the Westinghouse Engineering Achievement Award for the "Design and Fabrication of High Efficiency Silicon Solar Cells."

Rajeewa Arya, photograph and biography not available at the time of publication.